

## Polyphosphazene Electrolytes. 2. Synthesis and Properties of New Polymer Electrolytes Based on Poly((amino)[(2-methoxyethoxy)ethoxy])phosphazenes

Y. W. Chen-Yang,\* J. J. Hwang, and A. Y. Huang

Department of Chemistry, Chung Yuan Christian University, Chung-Li, Taiwan 32023, R.O.C.

Received July 6, 1999; Revised Manuscript Received November 2, 1999

**ABSTRACT:** A series of ether group and amino group cosubstituent phosphazene copolymers was synthesized and characterized by a combination of NMR, elemental analysis, and FTIR spectroscopy. The length of the alkyl group in the amino side chain and the content of the methoxyethoxyethoxy (MEE) substituent on the polymer properties were varied. Dynamic mechanical analysis (DMA) demonstrated that the cosubstituent polymers prepared have better mechanical properties than the ether homopolyphosphazene, poly[bis(2-methoxyethoxy)ethoxy]phosphazene, MEEP. The copolymers that possessed multiple electron-donor coordination sites, nitrogen and oxygen atoms, were complexed with various amounts of lithium perchlorate ( $\text{LiClO}_4$ ) to form polymer electrolytes. The ionic conductivity of the polymer electrolytes were determined by an impedance analyzer in a temperature range of 30–80 °C. According to those results, the conductivities of the prepared polymer electrolytes increased according to the rise in the MEE side chain contents and reached optima at  $F = 0.2\text{--}0.25$ . The best conductivity obtained is  $2.2 \times 10^{-5} \text{ S/cm}$  for CPE-3A with  $F = 0.25$ .

### Introduction

Solid polymer electrolytes (SPEs) received considerable attention in the early 1970s as many researchers attempted to produce a polymer-based electrolyte material with a high ionic conductivity that is mechanically and electrochemically stable. Wright et al. (1973) reported that poly(ethylene oxide) (PEO) and KSCN form a crystalline, stoichiometric polymer–salt complex.<sup>1</sup> Armand et al. (1978) recognized that solvent-free polymer–salt complexes might be excellent electrolytes for high-energy and -density solid-state batteries.<sup>2</sup> Since then, PEO has been studied extensively for use as an ionically conducting SPE. While attempting to ascertain the basic properties of the SPE matrix, these studies revealed that the crystallinity of PEO was not suitable for use as a polymer matrix of SPE because the operational temperature for most SPE applications is below the melting temperature of PEO. As a result, many researchers have attempted to modify the properties of PEO to eliminate any crystallinity.<sup>3–12</sup> However, an easier means of ascertaining useful polyether-based electrolytes is to utilize polymer blends and composites, in which high molecular weight polymers or inorganic (ceramic) powders were added to the polyether alkali metal salt complex.<sup>13,14</sup>

The ability of chemists to tailor the macroscopic properties of polyphosphazenes by incorporating various side groups was the basis for the belief that specific phosphazene derivatives might be useful in the area of SPEs. Blonsky et al. (1984) found that salt complexes of polyphosphazene with a pendant polyether side chain (MEEP) have significant ionic conductivity.<sup>15</sup> MEEP is amorphous at room temperature and below and functions as an excellent solid solvent for metal salts such as  $\text{LiSO}_3\text{CF}_3$  and  $\text{AgSO}_3\text{CF}_3$ . The conductivity of these MEEP–salt electrolyte systems at room temperature is 2–3 orders of magnitude larger than that of similar PEO salt complexes. However, poor mechanical stability inhibits the practical application of MEEP. The chemical

cross-linking of MEEP with poly(ethylene glycol) or the irradiation of either MEEP or  $\text{MEEP}-(\text{LiX})_{0.25}$  complexes with various doses of  $^{60}\text{Co}$   $\gamma$ -ray, or the use of a porous, fiberglass matrix to support MEEP have all been utilized to solve this problem.<sup>16</sup> Abraham et al. indicated that free-standing thin films with a slightly lower conductivity than that of  $\text{MEEP}-(\text{LiX})_n$  can easily be cast from a system composed of  $(\text{LiX})_n$  with a blend of MEEP and high molecular weight PEO.<sup>17,18</sup> Although recent reports indicate that the conductivity of the cosubstituent polyphosphazene of (methoxyethoxy)-ethoxy and poly(ethylene glycol)methyl ether exceeds that of MEEP, the dimensional stability of this polymer is not better than that of MEEP.<sup>19–21</sup> Nevertheless, the polyphosphazenes bearing branched oligoethylene side groups showed higher dimensional stabilities than MEEP.<sup>22</sup>

Our previous work involving a series of new polymer electrolytes based on poly[bis(amino)phosphazene] and  $\text{LiClO}_4$  showed satisfactory dimensional stability and ionic conductivity, but the ionic conductivity of the polymer electrolytes still did not reach the range needed for a rechargeable lithium battery.<sup>23</sup> In this study, we synthesized a series of [2-(2-methoxyethoxy)ethoxy]-(alkylamino) cosubstituent polyphosphazenes, with ethyleneoxy and amino side chains, that have potential sites for complexing or solvating the metal salts and dimensional stability. The properties of the new SPEs and the effect of the MEE side chain and the length of the amino group on the SPEs properties are discussed.

### Experimental Section

**1. Materials.** Hexachlorocyclotriphosphazene was kindly provided by the Nippon Fine Chemical Corp. Propylamine, butylamine, pentylamine, hexylamine, and triethylamine were purchased from the Merck Chemical Co., while lithium perchlorate ( $\text{LiClO}_4$ ), sodium hydride ( $\text{NaH}$ ), 2-(2-methoxyethoxy)ethanol, tetrahydrofuran (THF), sulfur ( $\text{S}_8$ ), benzene, and methanol were purchased from the Aldrich Chemical Co.. The reagents and the solvents were dried prior to use.

Scheme 1

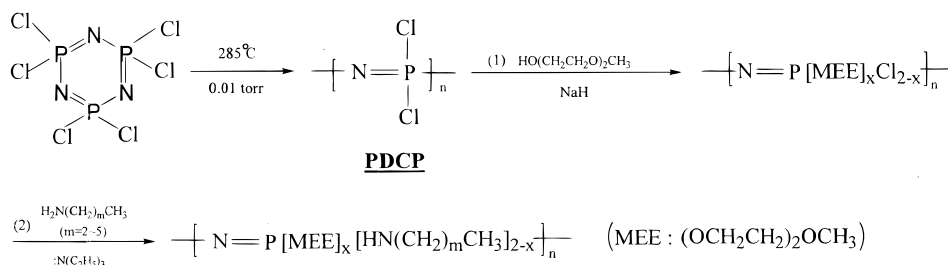
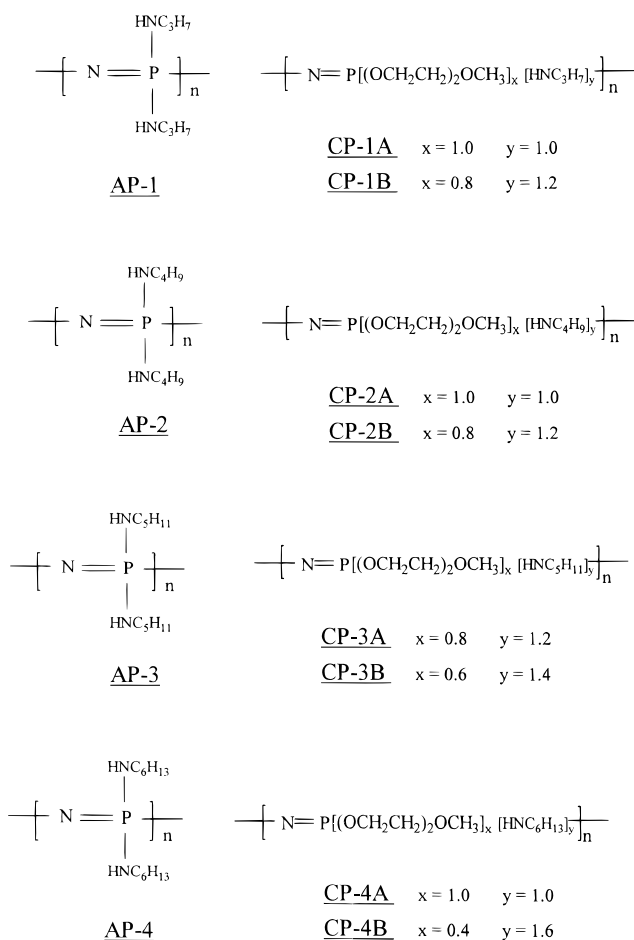


Chart 1



## 2. Synthesis of Poly[di(chloro)phosphazene] (PDCP).

The  $(\text{N}(\text{PCl}_2)_2)_n$  (PDCP) polymers were prepared according to the method reported.<sup>24</sup> Hexachlorotriphosphazene (50.0 g) and sulfur (5.0 g) were weighed directly by a Pyrex ampule, placed in a furnace, and heated at 285°C until the clear melting mixture became highly viscous but still slightly mobile. The ampule was opened, and the contents were extracted with dry benzene. The product, linear polymer  $(\text{N}(\text{PCl}_2)_2)_n$  (PDCP) was purified by precipitation from benzene solution into *n*-hexane, and 30.0 g of PDCP was obtained.

**3. Synthesis of Amino- and MEE-Containing Polyphosphazenes.** The mixed-substituent polyphosphazenes (CP-1–CP-4) (see Scheme 1 and Chart 1) were synthesized as follows: a solution of PDCP dissolved in THF was allowed to react at room temperature with the desired stoichiometric equivalence of sodium alkoxide for the first side group (MEE). This intermediate was then reacted with an excess of the second nucleophile, amine. All of the polyphosphazenes were prepared in a similar manner. To prepare CP-1A, freshly distilled 2-(2-methoxyethoxy)ethanol (6.20 g, 0.0517 mol) was added to a solution of sodium hydride (1.31 g/95%, 0.0517 mol) in THF (200 mL) to prepare MEENa. After 3 h of heating and

stirring in dry nitrogen, the sodium salt mixture was added dropwise to a solution of PDCP (10.5 g, 0.086 mol) in THF (500 mL). This mixture was further heated and stirred for 24 h in an atmosphere of dry  $\text{N}_2$  to obtain the partially MEE-substituted polyphosphazene. Freshly distilled propylamine (21.36 g/0.362 mol) and triethylamine (18.28 g/0.181 mol) were mixed in THF (150 mL) in a separate reaction vessel. The mixtures was added dropwise to the previously prepared partially substituted polyphosphazene solution and heated at reflux for 24 h, and THF was removed by a rotary evaporator. Excess methanol was then added to precipitate the polymer product. The residual amine hydrochloride salt and sodium salt were removed by several washings with methanol. The residual product was finally dried under a vacuum to obtain the cosubstituent polymer, CP-1A (13.8 g, 65% yield).

**4. Preparation of the Polymer Electrolytes.** The concentration of  $\text{LiClO}_4$  in the polymer electrolytes is expressed as the molar ratio of salt to monomeric unit of the polyphosphazene,  $F = [\text{MX}]/[\text{PN}]$ . Polymer electrolytes were prepared by dissolving the desired amount of  $\text{LiClO}_4$  in THF and mixing it with a THF solution of the polymer. The resulting mixture was stirred until a homogeneous solution was obtained. Upon removal of the solvent, the polymer electrolyte was dried under a vacuum at 40 °C for 48 h and then stored in a dry inert atmosphere before preparation of the corresponding films. The films were obtained by heating and compression of the polymer between two stainless plates which resulted in electrolyte membranes around 0.1–0.2 mm thick.

**5. Instruments.** The FTIR spectra were recorded on a Biorad-Digilab FTS-7. The samples were sandwiched between KBr windows.  $^1\text{H}$  and  $^{31}\text{P}$  NMR spectra were recorded on a Bruker AC 200 spectrometer using 85%  $\text{H}_3\text{PO}_4$  as an external reference for  $^{31}\text{P}$  NMR. The dynamic mechanical analysis (DMA) was performed on a Perkin-Elmer DMA. DSC and TGA measurements were performed on a Seiko DSC 200 and a Seiko TG/DTA 220, respectively. Ionic conductivities of the polymer electrolytes were determined by the complex impedance method using an HP4192A impedance analyzer over a frequency range of 5 Hz to 13 MHz.

## Results and Discussion

**Characterization of the Cosubstituent Polyphosphazenes (CP).** The cosubstituent polyphosphazenes (CP-1–CP-4) were synthesized by a two-step substitution reaction from PDCP, as depicted in Scheme 1. The PDCP was partially substituted with the MEE side chain first by reaction of PDCP with the sodium salt of the MEE alcohol and then the remaining chlorine atoms were substituted by reaction of the partially substituted polyphosphazene,  $\text{NP}(\text{MEE})_x\text{Cl}_{2-x}$ , with the selected amine.

Cosubstituent polymers with different substituents ratio were obtained by controlling the feed ratio of MEE alcohol and the amine. The structures of the cosubstituent polymers prepared were characterized by a combination of FTIR and  $^{31}\text{P}$  and  $^1\text{H}$  NMR spectroscopies and elemental microanalysis. The substitution reactions were monitored by the  $^{31}\text{P}$  NMR measurements. The PDCP  $^{31}\text{P}$  NMR spectrum showed only one peak at

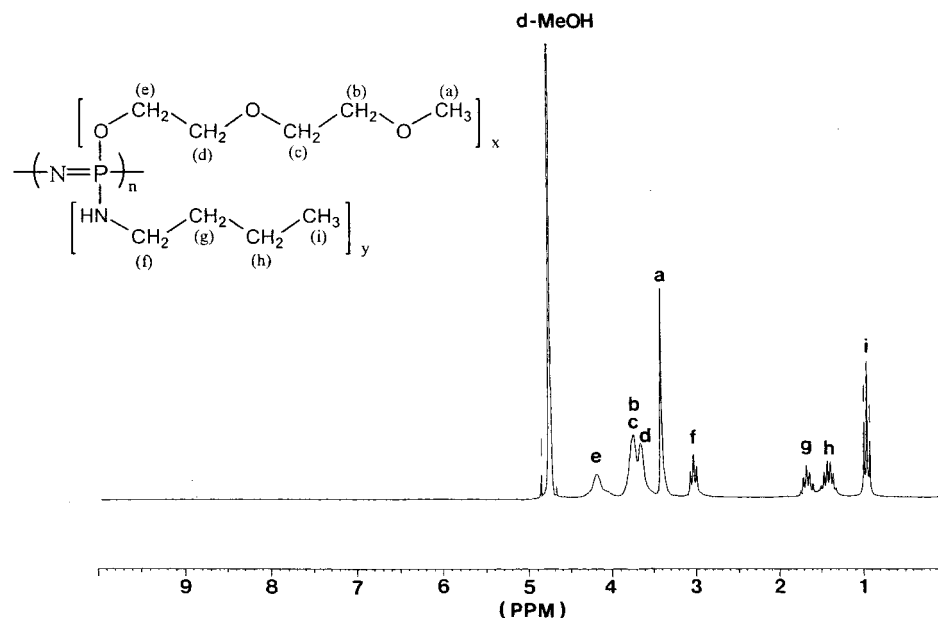


Figure 1.  $^1\text{H}$  NMR spectrum of CP-2A in  $d$ -MeOH solvent

Table 1.  $^1\text{H}$  NMR Characterization Data and Element Analysis Data for  $\{\text{NP}[\text{OCH}_2\text{CH}_2\text{OCH}_2\text{CH}_2\text{OCH}_3]_x[\text{HN}(\text{CH}_2)_m\text{CH}_3]_y\}_n$

polymer	$m$	$x$	$y$	$^1\text{H}$ NMR, ppm		elemental anal. (%)			
						N	C	H	% Cl
MEEP		2.0	0	3.4, 3.6, 3.7, 4.1	calcd	4.95	42.4	7.77	0
					found	4.95	40.62	7.76	<0.01
AP-1	2	0	2.0	0.86, 1.2–1.5, 2.80	calcd	26.1	44.7	9.90	0
					found	25.9	44.0	9.80	<0.01
AP-2	3	0	2.0	0.86, 1.2–1.5, 2.80	calcd	22.2	50.8	10.6	0
					found	22.0	49.9	10.4	<0.01
AP-3	4	0	2.0	0.85, 1.2–1.5, 2.85	calcd	19.4	55.3	11.1	0
					found	19.4	54.4	11.0	<0.01
AP-4	5	0	2.0	0.85, 1.2–1.5, 2.85	calcd	17.1	58.8	11.4	0
					found	17.2	57.9	11.2	<0.01
CP-1A	2	1.0	1.0	0.82, 1.22, 1.42, 2.77/3.21, 3.41, 3.52, 3.99	calcd	12.6	43.2	8.56	0
					found	12.8	43.3	8.58	<0.01
CP-1B	2	0.8	1.2	0.83, 1.45, 2.78/3.29, 3.43, 3.56, 3.93	calcd	14.7	43.5	8.77	0
					found	14.9	43.5	8.80	<0.01
CP-2A	3	1.0	1.0	0.87, 1.35, 2.80/3.34, 3.49, 3.61, 3.93	calcd	11.9	45.8	8.90	0
					found	12.3	46.0	8.97	<0.01
CP-2B	3	0.8	1.2	0.84, 1.29, 1.37, 2.8/3.24, 3.43, 3.53, 3.91	calcd	13.6	46.6	9.18	0
					found	13.4	46.5	9.14	<0.01
CP-3A	4	0.8	1.2	0.8, 1.2, 1.4, 2.8/3.3, 3.5, 3.6, 4.0	calcd	12.7	49.3	9.53	0
					found	12.5	49.2	9.50	<0.01
CP-3B	4	0.6	1.4	0.8, 1.2, 1.4, 2.8/3.3, 3.5, 3.6, 4.0	calcd	14.2	50.7	9.88	0
					found	13.8	50.3	9.79	<0.01
CP-4A	5	1.0	1.0	0.78, 1.2, 2.79/3.2, 3.41, 3.52, 4.0	calcd	10.6	50.0	9.47	0
					found	10.3	49.6	9.38	<0.01
CP-4B	5	0.4	1.6	0.8, 1.2, 1.4, 2.8/3.2, 3.5, 3.6, 4.0	calcd	14.4	55.1	10.6	0
					found	14.2	55.6	10.7	<0.01

–18.2 ppm as expected, and this peak disappeared after the first step of the substitution reaction. A combination of several sets of second-order coupling peaks representing  $\text{P}(\text{OR})\text{Cl}$  and  $\text{P}(\text{OR})_2$  were observed between +3 and –14 ppm indicating random substitution. After the second step of the substitution reactions, a simpler broad peak between 8 and 4 ppm was observed, revealing that the amino group had substituted the rest of the chlorine atoms. This was confirmed by the elemental microanalysis, in which a very small amount (<0.01) of the residual chlorine in the polymers was detected.

A ratio of the two side chains in each polymer substituted unit was determined by  $^1\text{H}$  NMR and elemental microanalysis data. The integration of the signal representing the MEE side chain was compared to the signal representing the amino side chain for the  $^1\text{H}$  NMR spectra. All of the  $^1\text{H}$  NMR spectra for the

cosubstituent polymers show two sets of peaks for CP-2A as illustrated in Figure 1. The peak between 4.0 and 3.3 ppm represents the protons of the MEE group while the second peak between 2.8 and 0.8 ppm represents the protons of the butylamino group. These two sets of well-separated peaks provide a satisfactory estimate of the ratio of the two substituent groups and confirm the ratio calculated from the elemental analysis. The  $^1\text{H}$  NMR and the elemental analysis data are summarized with substituent ratios in Table 1.

The chemical structures of the cosubstituent polymers are identified by comparing the FTIR spectra for the single-substituent polymers, AP-1–AP-4, with that for the cosubstituent polymers. The FTIR spectra for polymer MEEP, CP-1A, CP-1B, and AP-1 are shown in Figure 2. For polymer CP-1A, the peaks for the  $\text{P}=\text{N}$  stretching of the backbone are found in the region

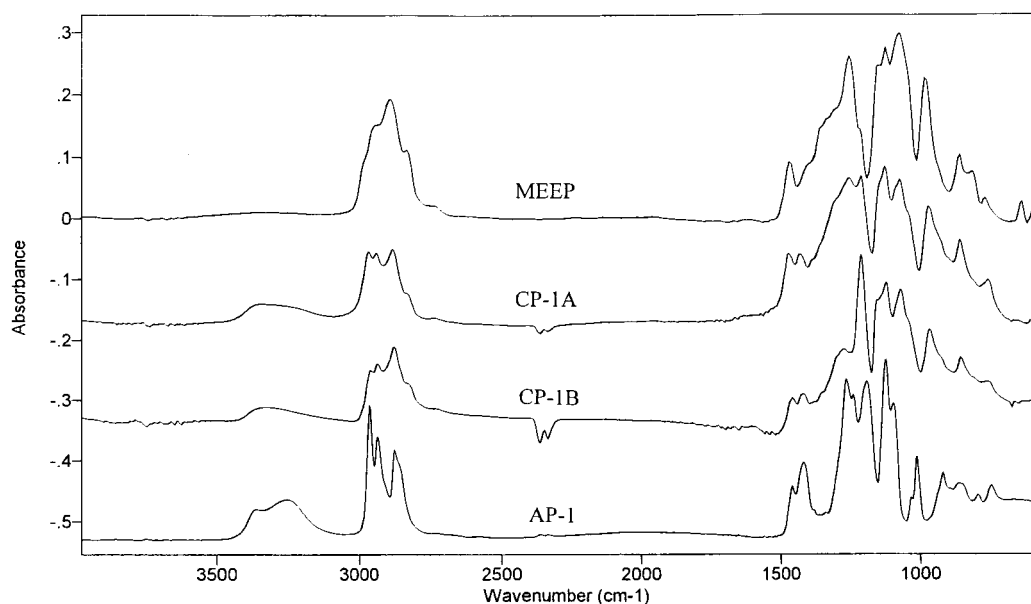


Figure 2. FTIR spectra of MEEP, CP-1A, CP-1B, and AP-1

Table 2. Characteristic Absorptions ( $\text{cm}^{-1}$ ) in FTIR Spectra of the Polymer

polymer	N-H	C-H	P=N	C-N	C-O-C	P-O-C	P-N-C
MEEP		2881, 1455	1242		1060	970	
AP-1	3367, 3251	2930, 1412	1260, 1234	1185, 1091			918
AP-2	3365, 3250	2928, 1412	1263	1189, 1094			917
AP-3	3353, 3253	2927, 1414	1257	1178, 1095			901
AP-4	3247, 3351	2924, 1412	1257	1180, 1095			902
CP-1A/CP-1B	3315	2900, 1430	1235	1185	1060	962	962
CP-2A/CP-2B	3270	2905, 1425	1230	1200	1060	962	962
CP-3A/CP-3B	3300	2928, 1459	1240	1201	1057	960	960
CP-4A/CP-4B	3255	2920, 1457	1245	1200	1060	960	960

$1230\text{--}1265\text{ cm}^{-1}$ , while the characteristic absorptions for the N-H stretching and the C-N stretching of the amino group are found in the regions  $3365\text{--}3250$  and  $1200\text{--}1090\text{ cm}^{-1}$  respectively. In addition, the absorptions for P-O-C and C-O-C stretching of the MEE group are found at  $940\text{--}1000$  and  $1100\text{--}1025\text{ cm}^{-1}$ , respectively. Similar spectra were obtained for the other cosubstituent polymers. Table 2 summarizes the characteristic absorptions.

**Thermal Properties of the Cosubstituent Polyphosphazenes.** The thermograms of the single-substituent polyphosphazenes, MEEP, and AP-1 and that of the corresponding cosubstituent CP-1A are shown in Figure 3. According to this figure, the propylamino group polymer AP-1 contains crystalline phases with a melting transition at  $149\text{ }^{\circ}\text{C}$ , which enhances the mechanical property but reduces conductivity. The flexible MEE side group polymer MEEP has a very low glass transition ( $-84\text{ }^{\circ}\text{C}$ ) and no melting transition. Therefore, MEEP appeared as a sticky material as expected, but AP-1 could be casted as a white translucent free-standing film. On the other hand, the cosubstituent polyphosphazene CP-1A is amorphous with a glass transition  $28\text{ }^{\circ}\text{C}$  higher than that of MEEP, indicating that the cosubstituent polyphosphazenes combines the flexibility of MEEP and the dimensional stability of AP-1.

The length and nature of the side groups influence the thermal behavior of the polyphosphazenes as summarized in Table 3. The polybisaminophosphazene, AP-2, contained crystalline phases while AP-3 and AP-4 were amorphous materials, however, for all of these phases material could be cast as free-standing films.

Table 3. Glass Transition Temperature ( $T_g$ ), Melting Point Temperature ( $T_m$ ) and Appearance of the Polymers

polymer	$T_g$ ( $^{\circ}\text{C}$ )	$T_m$ ( $^{\circ}\text{C}$ )	appearance
MEEP	-84		brown, sticky
AP-1		149	free-standing, white, translucent
AP-2		138	free-standing, transparent
AP-3	-2		free-standing, transparent
AP-4	-10		free-standing, transparent
CP-1A	-56.2		free-standing, yellow, translucent
CP-1B	-51.3		free-standing, yellow, translucent
CP-2A	-61.2		free-standing, yellow, translucent
CP-2B	-54.3		free-standing, yellow, translucent
CP-3A	-68.8		free-standing, yellow, translucent
CP-3B	-50.6		free-standing, yellow, translucent
CP-4A	-62.1		free-standing, yellow, translucent
CP-4B	-68.2		free-standing, yellow, translucent

All of the cosubstituent polymers were amorphous, and corresponding free-standing films were also obtained. This similarity can be ascribed to their glass transition temperatures, which were all  $30\text{ }^{\circ}\text{C}$  above that of MEEP indicating that the cosubstituents are more dimensionally stable than MEEP.

The  $T_g$  of the cosubstituent polymer with the same MEE content (e.g., CP-1A, CP-2A, CP-3A, and CP-4A) decreased with increasing length of the amino group because this also increased flexibility. The  $T_g$  of polymers with the same two substituents (e.g., CP-2A and CP-2B) increased as expected when the percentage of the MEE group was increased. However, the  $T_g$  of CP-4B was lower than that of CP-4A possibly because of the random orientation caused by longer chain of the hexylamino groups.

The thermal decomposition behaviors of MEEP, AP-1, and CP-1A are shown in Figure 4 to illustrate the

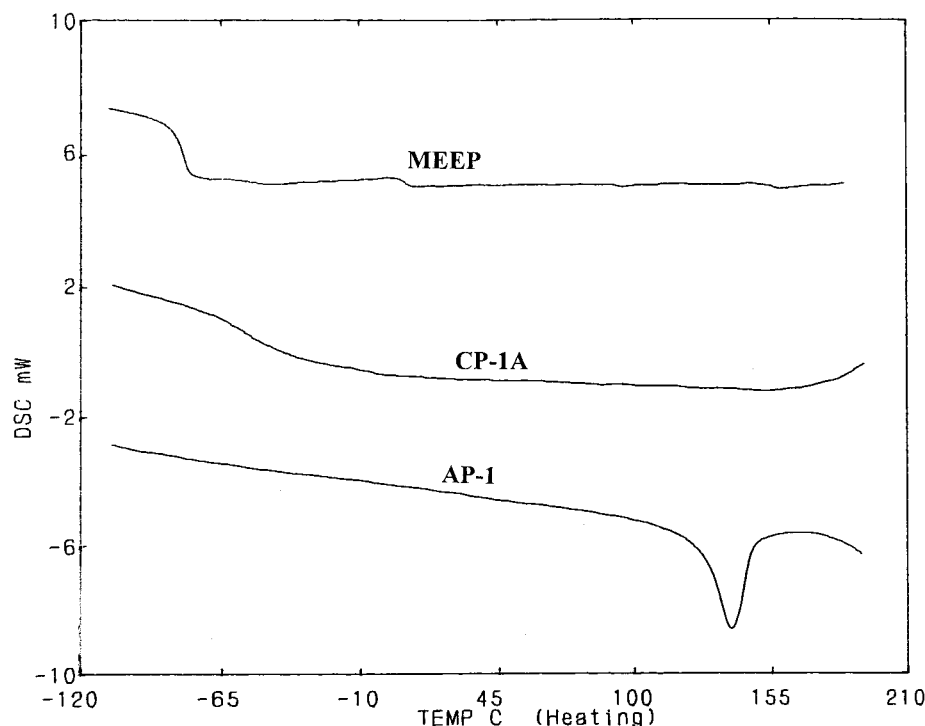


**Figure 3.** DSC heating curves recorded at 10 °C/min in the MEEP, CP-1A and AP-1

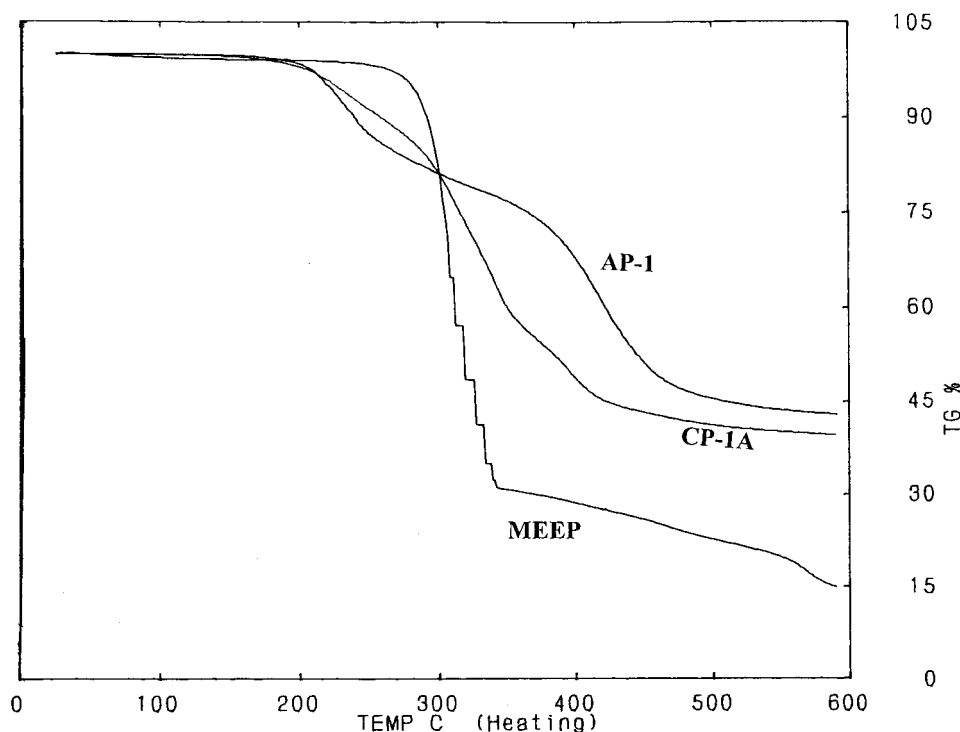


**Figure 4.** TGA heating curves of MEEP, CP-1A, and AP-1 behavior of two single-substituent polymers and that of the corresponding cosubstituent polymers. MEEP decomposed at  $T_{\max} = 327$  °C while AP-1 decomposed in two steps at  $T_{\max}$  at 248 and 423 °C, as summarized in Table 4. CP-1A, on the other hand, lost weight continuously above 200 °C with  $T_{5\%}$  and  $T_{\max}$  of 269 °C and 315 °C, respectively, indicating a combination of the decomposition behavior of MEEP and that of AP-1. This result indicates that the P–N bond connecting the amino group to the backbone of CP-1A is cleaved before the backbone P=N bond and the P–O bond connected the ethyleneoxy group to the backbone, during the

heating process. Similar results were found for the remaining cosubstituent polymers.

**Preparation and Thermal Properties of the Polymer Electrolytes (CPE).** The CP/LiClO<sub>4</sub> electrolytes (CPE) were prepared according to the procedures described above as depicted in Scheme 2. According to this scheme, all of the samples prepared were translucent homogeneous free-standing films with satisfactory dimensional stability. The CPE films prepared were dried and stored in a vacuum system since the LiClO<sub>4</sub>-containing CPEs were generally moisture sensitive. The FTIR spectra confirmed that the films were water-free.

Scheme 2

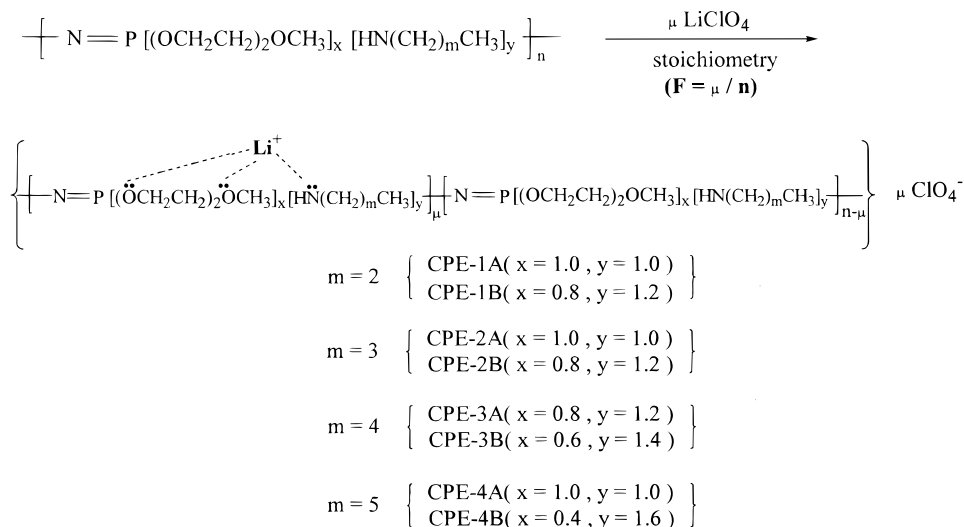


Table 4. Thermal Gravimetry Analysis Data of the Polymers

polymer	$T_{5\%}$ (°C) <sup>a</sup>	$T_{\max}$ (°C) <sup>b</sup>	char yield (%)
MEEP	282	327	14.8
AP-1	231	248/423	41.9
AP-2	228	242/429	33.5
AP-3	240	260/426.5	28.5
AP-4	233	263/428.2	25.7
CP-1A	269	315	30.7
CP-2B	219	326	32.3
CP-3A	178	278	28.9
CP-4A	209	330	24

<sup>a</sup> The temperature with 5% weight loss,  $T_{5\%}$  <sup>b</sup> The temperature at which the polymer's maximum rate of weight loss occurred,  $T_{\max}$

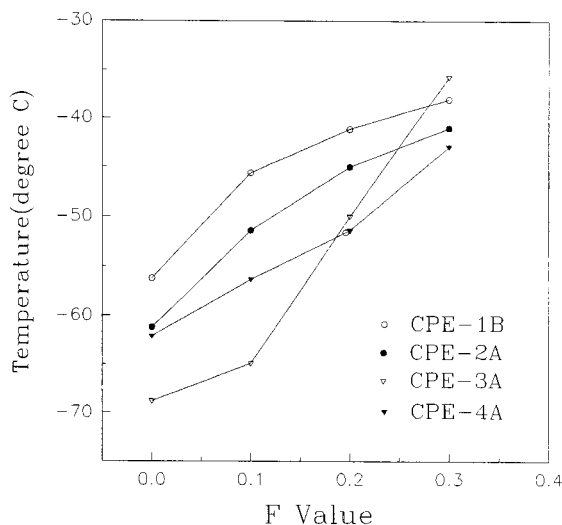
Table 5. The Glass Transition Temperature (°C) Values of the CPE vs the Content of LiClO<sub>4</sub>

sample	$T_g$			
	$F=0$	$F=0.1$	$F=0.2$	$F=0.3$
CPE-1A	-56	-46	-41	-38
CPE-2A	-61	-51	-45	-41
CPE-3A	-69	-65	-50	-36
CPE-4A	-62	-56	-51	-43

also found that with  $F=0.3$ ,  $T_g$ s of all the other CPEs are more than 20 °C above that of the corresponding parent polymers. The glass transition temperature data are summarized along with  $F$  values in Table 5. Better mechanical stability can be obtained for the CPEs than that for their parent polymers because of possible virtual cross-links between the lithium ion and the oxygen and/or the nitrogen atoms in the polymers.<sup>23, 25</sup>

The storage modulus ( $4.5 \times 10^{-8}$  Pa) and the  $T_g$  (-36.7 °C) (the peak temperature of  $T_{\text{and}}$ ) of CPE-3A with  $F=0.3$  were determined by the DMA measurement. Nevertheless, other films were not strong enough to be determined even though they were all free-standing. The  $T_g$  determined by the DMA was about the same as the value (-35.7 °C) determined by the DSC.

**Ionic Conductivity of the CPEs.** The ionic conductivity of the CPEs were measured by a complex impedance analysis. The cosubstituent polymers without lithium salt ranged in conductivity between  $3 \times 10^{-8}$  and  $5.5 \times 10^{-7}$  S/cm at room temperature as listed in Table 6. When LiClO<sub>4</sub> was added, the ionic conductivity ranged between  $5.3 \times 10^{-7}$  and  $2.2 \times 10^{-5}$  S/cm. This is much larger than that of the single substituted polyamino-phosphazene (AP-3 and AP-4) based electrolyte<sup>22</sup> and can be ascribed to the additional free volume generated by the uneven and random orientations of the cosubstituents in the polymers. The CPEs with a larger percentage of MEE side chains showed higher conductivity as expected. CPE-2A, CPE-3A, and CPE-4A with  $F=0.25$  had the maximum conductivity while the maximum conductivity occurred at  $F=0.2$  for CPE-1A as seen in Figure 6. In addition, the conductivity of the polymer electrolytes with the same  $F$  value at room-temperature ranged as follows: CPE-3A > CPE-4A > CPE-2A > CPE-1A. The maximum conductivity achieved in this study was  $2.2 \times 10^{-5}$  S/cm for CPE-3A with  $F=0.25$ , which is two orders higher than that for the AP/

Figure 5. Glass transition temperature values of the CPE vs the content of LiClO<sub>4</sub>

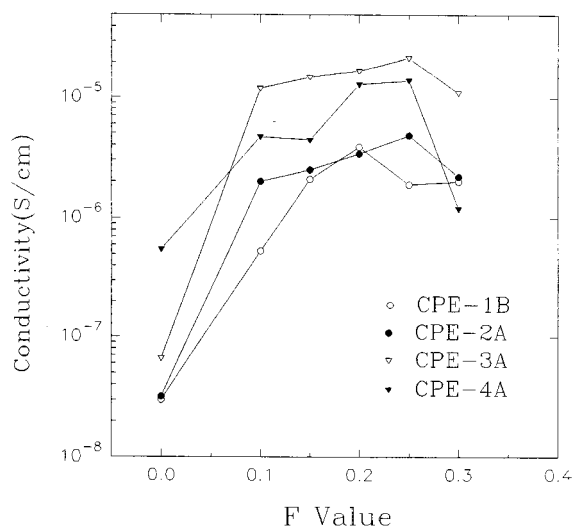
A DSC analysis of the CPE samples indicates that all of the CPEs are amorphous and LiClO<sub>4</sub> is miscible in the polymers because their thermograms show a single glass transition temperature without a melting transition. The glass transition temperatures for the CPE were selected with an increase in the content of LiClO<sub>4</sub>, as indicated by the  $F$  values depicted in Figure 5. For example, the  $T_g$  of CPE-3A range from -65 °C, for the sample with  $F=0.10$ , to -36 °C for the sample with the greatest loading ( $F=0.3$ ). In addition, it was

**Table 6. The Conductivities (S/cm) of the CPEs with Various  $F$  Values**

	$F = 0$	$F = 0.1$	$F = 0.15$	$F = 0.2$	$F = 0.25$	$F = 0.3$
CPE-1B	$3.0 \times 10^{-8}$	$5.3 \times 10^{-7}$	$2.1 \times 10^{-6}$	$3.9 \times 10^{-6}$	$1.9 \times 10^{-6}$	$2.0 \times 10^{-6}$
CPE-2A	$3.2 \times 10^{-8}$	$2.0 \times 10^{-6}$	$2.5 \times 10^{-6}$	$3.4 \times 10^{-6}$	$4.8 \times 10^{-6}$	$2.2 \times 10^{-6}$
CPE-3A	$6.6 \times 10^{-8}$	$1.2 \times 10^{-5}$	$1.5 \times 10^{-5}$	$1.7 \times 10^{-5}$	$2.2 \times 10^{-5}$	$1.0 \times 10^{-5}$
CPE-4A	$5.5 \times 10^{-7}$	$4.7 \times 10^{-6}$	$4.4 \times 10^{-6}$	$1.3 \times 10^{-5}$	$1.4 \times 10^{-5}$	$1.2 \times 10^{-6}$

**Table 7. The Conductivities (S/cm) of the CPEs ( $F = 0.2$ ) with Different Temperatures**

	$T = 303$	$T = 313$	$T = 323$	$T = 333$	$T = 343$	$T = 353$
CPE-1A	$5.67 \times 10^{-6}$	$1.36 \times 10^{-5}$	$2 \times 10^{-5}$	$4.47 \times 10^{-5}$	$7.2 \times 10^{-5}$	$1.26 \times 10^{-4}$
CPE-2A	$3.4 \times 10^{-6}$	$5.2 \times 10^{-6}$	$8 \times 10^{-6}$	$1.1 \times 10^{-5}$	$3.0 \times 10^{-5}$	$5.5 \times 10^{-5}$
CPE-3A	$1.7 \times 10^{-5}$	$3.9 \times 10^{-5}$	$6.3 \times 10^{-5}$	$8.4 \times 10^{-5}$	$1.3 \times 10^{-4}$	$1.7 \times 10^{-4}$
CPE-4A	$1.3 \times 10^{-5}$	$2.4 \times 10^{-5}$	$4.1 \times 10^{-5}$	$6.2 \times 10^{-5}$	$9.2 \times 10^{-5}$	$1.2 \times 10^{-4}$

**Figure 6.** Ionic conductivity with  $\text{LiClO}_4$  concentration in CPE series

$\text{LiClO}_4$  electrolytes and slightly below that for the MEEP/ $\text{LiClO}_4$  electrolytes.<sup>23</sup> This may be ascribed to the difference in the coordinative power toward lithium ions of the amino groups and that of the side group oxygens.

These observations confirm that the ionic conductivity of polymer electrolytes is affected by backbone flexibility revealed by the  $T_g$ , free volume of the side chains and the number of charge carrier as indicated by the  $F$  value.

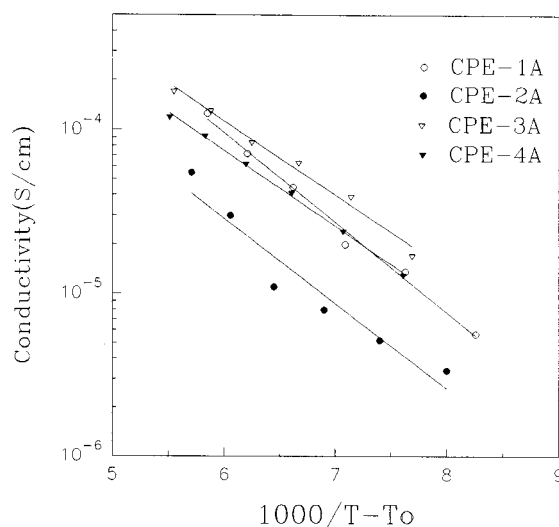
**Temperature Variation in Conductivity Behavior.** The temperature dependences of the ionic conductivity of the polymer electrolytes prepared in this study were measured from 30 to 80 °C, and the results are listed in Table 7. The conductivity ( $\sigma$ ) of amorphous polymer electrolytes declines exponentially when the temperature drops toward  $T_g$ , indicating that free volume plays a dominant role in the ion mobility. This may be explained by the empirical Vogel–Tamman–Fulcher (VTF) equation for fluidity of glass-forming liquids.

$$\sigma(T) = \sigma_0 \exp(-[B/(T - T_0)])$$

$$T_0 = T_g - 50$$

$T_0$  is the thermodynamic glass transition temperature and can be predicted by the Adams–Gibbs configurational entropy model.<sup>26, 27</sup>

Figure 7 indicates that the temperature dependence of the conductivity in the temperature range measured has good correspondence to the VTF approximation, revealing that the segmental movement and, therefore, the ionic mobilities may be explained by the simple

**Figure 7.** VTF-plotted approximation of conductivity vs reciprocal temperature in CPE electrolytes.  $F = 0.2$ .**Table 8. VTF Parameters of CPEs ( $F = 0.2$ ) Series**

	CPE-1A	CPE-2A	CPE-3A	CPE-4A
$B$ (K)	1264	1196	1043	1067
$\sigma$ (S/cm)	0.19	0.038	0.059	0.046
$T_0$ (K)	182	178	173	172

configurational entropy arguments. The preexponential factors,  $\sigma_0$ , and the pseudoactivation energies,  $B$ , obtained from the plots are listed in Table 8 along with  $T_0$  values.

## Conclusion

A series of mixed-substituent polyphosphazenes bearing (2-methoxyethoxy)ethoxy and alkylamine side groups were synthesized and characterized. These cosubstituent polymers are amorphous over a wide temperature range and are significantly more stable than the homopolymer MEEP. These cosubstituent polymers all have a glass transition temperature at  $-65$  to  $-50$  °C, which is 20–30 °C higher than the  $T_g$  of MEEP. The cosubstituent polymers form amorphous polymer electrolytes with the proper concentration of lithium perchlorate. The conductivity data indicated that salt complexes of the polymers with the higher percentage of MEE side chains gave a higher conductivity. All the polymer electrolytes showed an increase in conductivity with increasing salt concentration. In each system there was a maximum conductivity at a specific salt concentration. The use of MEE and alkylamino side chains produced free-standing films with ionic conductivity of  $10^{-5}$ – $10^{-6}$  S/cm at room temperature for the CPE/ $\text{LiClO}_4$  polymer electrolytes. The temperature dependence of

the conductivity between 30 and 80 °C has satisfactory correspondence to the VTF approximation. The greatest conductivity of  $2.2 \times 10^{-5}$  S/cm at room temperature and  $1.7 \times 10^{-4}$  S/cm at 80 °C was obtained for CPE-3A/LiClO<sub>4</sub> ( $F=0.25$ ). This may prove to be a useful solid polymer electrolyte for rechargeable batteries.

**Acknowledgment.** The authors would like to thank the National Science Council of the Republic of China for financially supporting this research under Contract No. NSC86-2113-M-033-004.

## References and Notes

- (1) Fenton, D. E.; Parker, J. M.; Wright, P. V. *Polymer* **1973**, *14*, 589.
- (2) Armand, M. B.; Chabagno, J. M.; Duclot, M. J. *Abstracts of Papers, Second International Meeting on Solid Electrolytes, St. Andrews, Scotland*; 1978; p 65.
- (3) Ratner, M. A.; Shriver, D. F. *Chem. Rev.* **1988**, *88*, 109.
- (4) Blonsky, P. M.; Clancy, S.; Hardy, L. C.; Harris, C. S.; Spindler, R.; Tonge, J. S.; Shriver, D. F. *CHEMTECH* **1987**, 758.
- (5) Shriver, D. F.; Farrington, G. C. *Chem. Eng. News* **1985**, *63*, 3 (20), 42.
- (6) Foos, J. S.; Erker, S. M. *J. Electrochem. Soc.* **1987**, *134*, 1724.
- (7) Goulart, G.; Sylla, S.; Sanchez, J. V. In *Second international Symposium on Polymer Electrolytes*; Scrosati, B., Ed.; Elsevier Applied Science: London, 1990.
- (8) Giles, J. R.; Booth, C.; Mobbs, R. H. In *Proceedings of the 6<sup>th</sup> Riso International Symposium on Metallurgy and Materials Science*; Poulsen, F. W.; Anderson, N. H.; Clausen, K.; Skaarup, S.; Sorensen, O. T., Eds.; Riso National Laboratory: Roskilde, Denmark, 1985.
- (9) Craven, J. R.; Mobbs, R. H.; Booth, C.; Giles, J. R. M. *Makromol. Chem., Rapid Commun.* **1986**, *7*, 81.
- (10) Nicholas, C. V.; Wilson, D. J.; Booth, C.; Giles, J. R. M. *Br. Polym. J.* **1988**, *20*, 289.
- (11) Linden, E.; Owen, J. R. *Solid State Ionics* **1988**, *28*, 994.
- (12) Gray, F. M. *Solid State Ionics* **1990**, *40/41*, 637.
- (13) Appetechchi, G. B.; Dautzenberg, G.; Scrosati, B. *J. Electrochem. Soc.* **1996**, *143*, 6.
- (14) Scrosati, B.; Croce, F. *Polym. Adv. Technol.* **1993**, *4*, 198.
- (15) Blonsky, P. M.; Shriver, D. F.; Austin, P.; Allock, H. R. *J. Am. Chem. Soc.* **1984**, *106*, 6854.
- (16) Allcock, H. R. *Chem. Mater.* **1994**, *6*, 1476.
- (17) Abraham, K. M.; Alamgir, M. *J. Power Source* **1993**, 43–44, 195.
- (18) Abraham, K. M.; Alamgir, M.; Reynolds, R. K. *J. Electrochem. Soc.* **1989**, *136*, 3576.
- (19) Allcock, H. R.; Napierala, M. E.; Cameron, C. G.; O'Connor, S. J. M. *Macromolecules* **1996**, *29*, 1951.
- (20) Allcock, H. R.; Kuharcik, S. E.; Reed, C. S. Napierala, M. E. *Macromolecules* **1996**, *29*, 3384.
- (21) Allcock, H. R.; Olmeijer, D. L.; O'Connor, S. J. M. *Macromolecules* **1998**, *31*, 753.
- (22) Allcock, H. R.; O'Connor, S. J. M.; Olmeijer, D. L.; Napierala, M. E.; Cameron, C. G. *Macromolecules* **1996**, *29*, 7544.
- (23) Chen-Yang, Y. W.; Hwang, J. J.; Chang, F. H. *Macromolecules* **1997**, *30*, 3825.
- (24) Kajiwar, M.; Moriya, K.; Tomii, K.; Yano, S. *Makromol. Chem.*, **1992**, *193*, 435.
- (25) Lee, J.; Khan, I. M. *Macromolecules* **1993**, *26*, 4544.
- (26) Adam, G.; Gibbs, J. H. *J. Chem. Phys.* **1965**, *43*, 139.
- (27) Bruce, P. G.; Vincent, C. A. *J. Chem. Soc., Faraday Trans.* **1993**, *122*, 131.

MA991080Y